Iğdır Üniversitesi Fen Bilimleri Enstitüsü Dergisi, 12(4): 2340 - 2351, 2022
Journal of the Institute of Science and Technology, 12(4): 2340 – 2351, 2022
ISSN: 2146-0574, eISSN: 2536-4618
Kimya / *Chemistry* **DOI: 10.21597/jist.1145142**
Araştırma Makalesi / *Research Article*
Geliş tarihi / *Received*: 18.07.2022 **Kabul tarihi / *Accepted*: 09.11.2022**

Atıf İçin: Altun K, Yıldıko Ü, Tanrıverdi A A, Tekeş A T, Ata A Ç, Kartal B, Çakmak İ, 2022. 4-(5-metil-[1, 2, 4] triazolo [1, 5-a] pirimidin-7-iloksi) ftalonitrilin Yapısal ve Spektral Özellikleri: TD-DFT Yöntemi ile Analizi, ADME Analizi ve Moleküler Doking Simülasyonları. Iğdır Üniversitesi Fen Bilimleri Enstitüsü Dergisi, 12(4): 2340 - 2351.

To Cite: Altun K, Yıldıko Ü, Tanrıverdi A A, Tekeş A T, Ata A Ç, Kartal B, Çakmak İ, 2022. Structural and Spectral Properties of 4-(5-methyl-[1, 2, 4] triazolo [1, 5-a] pyrimidine-7-yloxy) phthalonitrile: Analysis by TD-DFT Method, ADME Analysis, and Molecular Docking Simulations. Journal of the Institute of Science and Technology, 12(4): 2340 - 2351.

4-(5-metil-[1, 2, 4] triazolo [1, 5-a] pirimidin-7-iloksi) ftalonitrilin Yapısal ve Spektral Özellikleri: TD-DFT Yöntemi ile Analizi, ADME analizi ve Moleküler Doking Simülasyonları

Kenan ALTUN[1], Ümit YILDIKO[1], Aslıhan Aycan TANRIVERDİ[2*], Ahmet Turan TEKEŞ[2], Ahmet Çağrı ATA[2], Barış KARTAL[3], İsmail ÇAKMAK[2]

ÖZET: Bu çalışmada ftalonitril bileşiği ve kuantum kimyasalı olarak 4-(5-metil-[1,2,4]triazolo[1,5-a]pirimidin-7-iloksi)ftalonitril (MTPPN olarak kodlanmıştır) seçilmiştir ve in-siliko çalışmalar yapılmıştır. İlk başta zamana bağlı yoğunluk fonksiyonel teorisi (TD-DFT) yönteminin temel seti kullanılmış ve molekülün sınır yörünge enerjileri ve bant aralığı hesaplamaları yapılmıştır. Elektron yoğunluğu ve bağ kritik nokta hakkında bilgi edinmek için moleküllerdeki atomların analizi (AIM) teorik hesaplamaları sunulmaktadır. Ayrıca bileşiğin ilaç potansiyeli için absorpsiyon, dağılım, metabolizma ve atılım (ADME) analizleri yapıldı. MTPPN bileşiğinin bazı enzimler üzerindeki etkisi incelenmiştir. Yerleştirme puanı sırasıyla AChE, BChE, a-GLY proteinleri -7.864, -6.848 ve -5.511 kcal/mol için elde edilmiştir. MTPPN, bir ilaç adayı olarak in-siliko bir çalışmada iyi bir inhibitör performans göstermiştir.

Anahtar Kelimeler: Ftalonitril, moleküler doking, ADME, TD-DFT, AIM

Structural and Spectral Properties of 4-(5-methyl-[1, 2, 4] triazolo [1, 5-a] pyrimidine-7-yloxy) phthalonitrile: Analysis by TD-DFT Method, ADME Analysis, and Molecular Docking Simulations

ABSTRACT: In this study, 4-(5-methyl-[1,2,4]triazolo[1,5-a]pyrimidine-7-yloxy) phthalonitrile (coded as MTPPN) was chosen as the phthalonitrile compound and the quantum chemical and in-silico studies have been done. First, the basis set of the time dependent density functional theory (TD-DFT) method was used and the boundary orbital energies and band gap calculations of the molecule were performed. Analysis of atoms in molecules (AIM) theoretical calculations is presented to learn about electron density and bond critical point. In addition, absorption, distribution, metabolism, and excretion analyzes (ADME) were performed for the drug potential of the compound. On some enzymes effect of MTPPN compound was examined. The docking score was obtained for AChE, BChE, α-GLY proteins -7.864, -6.848, and -5.511 kcal/mol, respectively. MTPPN gave a good inhibitory performance in an in-silico study as a drug candidate.

Keywords: Phthalonitrile, molecular docking, ADME, TD-DFT, AIM

[1] Kenan ALTUN (**Orcid ID:** 0000-0001-7736-5700), Ümit YILDIKO (**Orcid ID:** 0000-0001-8627-9038), Kafkas Üniversitesi, Mühendislik ve Mimarlık Fakültesi, Biyomühendislik Bölümü, Kars, Türkiye
[2] Aslıhan Aycan TANRIVERDİ (**Orcid ID:** 0000-0001-5811-8253), Ahmet Turan TEKEŞ (**Orcid ID:** 0000-0002-9942-7367), Ahmet Çağrı ATA (**Orcid ID:** 0000-0002-2296-2265), İsmail ÇAKMAK (**Orcid ID:** 0000-0002-3191-7570), Kafkas Üniversitesi, Fen-Edebiyat Fakültesi, Kimya Bölümü, Kars, Türkiye
[3]Barış KARTAL (**Orcid ID:** 0000-0002-7227-4647), Adıyaman Üniversitesi, Gölbaşı Meslek Yüksekokulu, Madenlerde İş Güvenliği ve İşçi Sağlığı, Adıyaman, Türkiye
***Sorumlu Yazar/*Corresponding Author*:** Aslıhan Aycan TANRIVERDİ, e-mail: t.aslihanaycan@gmail.com
Bu çalışma Kenan ALTUN'un Yüksek Lisans tezinden üretilmiştir.

INTRODUCTION

Phthalonitrile compounds are versatile 4-macrocyclic compounds that use as precursors for phthalocyanine and other pigments, fluorescent brighteners, and photographic sensitizers (Nemykin et al., 2010). These composites and materials offer important properties for applications in many fields such as industry, electronic material quality improvement, aviation, and maritime. Synthesis of symmetrical or unsymmetrical MPcs by modification of phthalonitriles has been used in many studies (Pathak et al., 2021; Priya Madhuri et al., 2022). Phthalonitriles are used to prepare composite materials and improve material properties. These studies include the addition of polymer matrix, doping of flame retardant, fluorescent sensing, and photosensitizing properties (Madakbaş et al., 2013; Ilyas et al., 2021; Yang et al., 2021).

NLO-type materials are classified as semiconductor structures or inorganic compounds. These structures have certain nonlinear optical properties because they can be hyperpolarized (LEDOUX et al., 1994; HASHIMOTO et al., 2001; Mendiratta et al., 2015). Optoelectronics is a rapidly growing technology, especially in the communication sector, and its importance in our lives is increasing day by day (Liu et al., 2021). Some application areas where optoelectronics have entered our lives and changed our way of life have become important in many areas such as barcode readers, the entertainment industry, magnetic recording media, defense industry, communication industry, and the health sector (Oida 2006). Density functional theory (DFT) and time dependent density functional theory (TD-DFT) excels in theoretical modeling. With this technique, it is used to determine the interaction properties of molecules in biological and chemical systems and to calculate many important chemical and physical properties (van Mourik et al., 2014; Zangwill 2014). The synthesis of phthalonitrile is given Figure 1 (Ağirtaş et al., 2017).

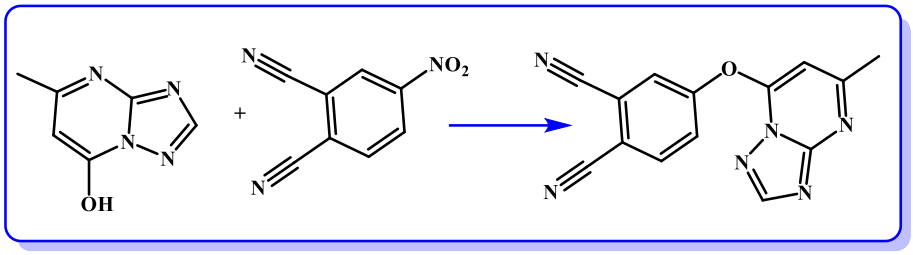

Figure 1. Synthetic route to the compound (Ağirtaş et al., 2017)

In this study, the electronic structure of the molecule, energy levels, and various chemical parameters were calculated by DFT analysis. Some thermodynamic parameters, potential energy maps, HOMO-LUMO energy levels, and Fukui function of the title compound were calculated. The chemical bonds are characterized as theoretical via AIM analysis and enzyme inhibitor properties were carried out as drug candidates with the pharmacokinetic analysis.

MATERIALS AND METHODS

Computational Methods

Molecular quantum chemical and drug potential studies

The MTPPN molecule was calculated with the DFT/B3LYP method via the TD-DFT/LanL2DZ and 6-311G (d,p) basis set in the Gaussian 09 program (Frisch and et al., 2016). The topology analysis was carried out in the AIMAII program (Pendás and Gatti, 2021). Online servers just as SwissADME were used for ADME analysis (Daina and et al., 2017). Molecular docking study for ligand-enzyme interactions and the compound's potential to bind to protein as an inhibitor was performed with Schrödinger's Maestro Molecular Modeling (version 11.8) platform (Madhavi and et al., 2013). The

crystal structures of human acetylcholinesterase (AChE) (PDB code:4M0E), butyrylcholinesterase (BChE) (PDB code:6SAM) and alpha-glucosidase (α-GLY) (PDB code:3A4A) enzymes were downloaded from PDB database (Altun and et al., 2021; Dong and et al., 2021; Tekes and et al., 2021). Preparation and ligand docking placement studies were carried out using ligprep module, protein prep, and receptor grid box modules. Inhibition performance, docking score, and binding conformations were determined. Docking study results were envisioned (Visualizer 2005) with the Discovery Studio 2016 client (BIOVIA Discovery Studio, 2016).

RESULTS AND DISCUSSION

TD-DFT and DFT Studies

Frontier molecular orbitals of MTPPN

For electrical parameters formed by electrons in a molecule and presented by molecular orbitals, HOMO and LUMO and energy are the band gaps (De Lile et al., 2020). The outermost orbitals filled with electrons are HOMO and the vacant orbitals that can receive electrons in intramolecular electron transfer, while the LUMO orbitals state the interplay of the molecule with other sorts (Yankova et al., 2016). The volume orbit of HOMO and LUMO for molecules is shown in Figure 2. In addition, LUMO + 1 and HOMO-1 graphs of the compound were taken. From Table 1, HOMO -4.236 eV—LUMO -2.154 eV was found in the calculation by DFT/ B3LYP/ 6-311G (d,p) basis set for the MTPPN compound, and HOMO -4.208 eV—LUMO -2.106 eV in the calculation made by the TD-DFT/LanL2DZ/6-311G level. Band Gap (Δ) = $|E_{HOMO} - E_{LUMO}|$ calculated by DFT and TD-DFT method, values of 2.082 eV and 2.102 eV were obtained, respectively. Therefore, HOMO-LUMO energy values and Band Gap values are quite close to each other. This is because the energies contribute to the same electronic region. In this case, as a result of the calculation of the HOMO-LUMO energies and other parameters, the electronic properties of the MTPPN compound were determined by the small group approach. With the energy maps of the molecular structure, the kinetic equilibrium and chemical reactivity values of the molecule in chemical reactions or intramolecular interactions can be calculated from the orbitals. The chemical softness of the molecule will allow it to be excited with lower energies. Other parameters obtained in the calculations are given in Table 1. It is thought that the obtained parameter for the obtained phthalonitrile is a soft molecule and can easily be polarized.

Table 1. Energy parameters for MTPPN

Molecular Energy	DFT	TD-DFT
E_{LUMO}	-2.154	-2.106
E_{HOMO}	-4.236	-4.208
E_{LUMO+1}	-1.536	-1.471
E_{HOMO-1}	-7.165	-7.359
Band Gap $\Delta = \|E_{HOMO} - E_{LUMO}\|$	2.082	2.102
Ionization Potential ($I = - E_{HOMO}$)	4.236	4.208
Electron Affinity ($A = - E_{LUMO}$)	2.154	2.106
Chemical hardness ($\eta = (I - A)/ 2$)	1.041	1.051
Chemical softness ($s = 1/2\ \eta$)	0.48	0.475
Chemical potential ($\mu = - (I + A)/ 2$)	-3.195	-3.155
Electronegativity ($\chi = (I+ A)/ 2$)	3.195	3.155
Electrophilicity index ($\omega= \mu^2 / 2\ \eta$)	4.903	4.735

Herein, the HOMO, which can be like the outer orbital containing electrons, tends to donate these electrons as electron donors, and hence the ionization potential is directly related to the energy of the HOMO. On the other hand, LUMO can accept electrons and LUMO energy is directly related to electron

affinity. Two important molecular orbitals were investigated for MTPPN, HOMO and LUMO, given in Figure 2.

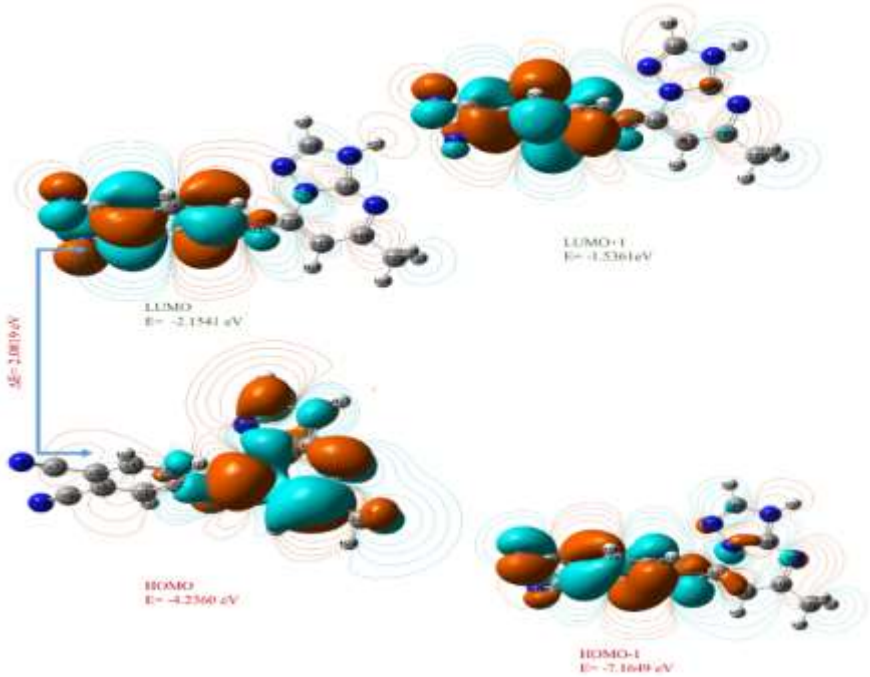

Figure 2. Frontier orbital energy maps for MTPPN with DFT in the UV-Visible region

Fukui function

Fukui functions were calculated to predict attack sites in the compounds. The cation position and anion position of the compound are considered as the Fukui function, provided that the attack sites have an optimized and maximum condensed structure (Bulat et al., 2004) by the DFT technique. This function indicates the tendency and tendency of the electronic density to deform at an appropriate position on the accepting or donating phenomenon of the molecule's electrons. Fukui functions are explained with the following expression (Demircioğlu et al., 2015),

Electrophilic attack; $f_j^- = q_{j\,N0} - q_{j\,(N-1)}$

Nucleophilic attack; $f_j^+ = q_{j(N+1)} - q_{j\,N0}$

Radical attack; $f_j^o = (q_{j(N+1)} - q_{j\,(N-1)})/2$

Dual descriptor; $\Delta f(r) = f_j^+ - f_j^-$

Mulliken atomic charges are denoted by cationic (N-1), anionic (N+1), and neutral (N) chemical species in the atomic region. Here, sprawl with the radical, electrophilic and nucleophilic signs "0", "+", and "-", respectively. Table 2 presents the values of the MTPPN Fukui function calculated parameters f_j^+ +, f_{jo}, and f_j^- at the level of DFT theory with the B3LYP/6-311G basis set. When $\Delta f(r)$ is negative, the atom is electrophilic and when $\Delta f(r)$ is positive, the atom is nucleophilic. In the following order, the duplicate identifier for electrophilic attack is N21> N19> O7> N15> C2> C3> C9> C6> C13. Pairs that allow nucleophilic attack and are negative are listed as 8 N>16 C>12 C>1 C>20 C>14 C>18 C>4 C>5 C>17 N>11 C.

AIM analysis of MTPPN

Atoms in molecules (AIM) characterize chemical bonds. In this theory, the critical point (CP) and the bond path (BP) between atoms attached to chemical bonds are always accompanied. Each bond path critical point (BCP) contains well-done chemical information that fully describes the form of the chemical bond.

Table 2. Fukui function for the MTPPN

Atoms	Mulliken atomic charges			Fukui functions			
	$q_{(N+1)}$	q_{N0}	$q_{(N-1)}$	f_j+	f_j-	f_j0	$\Delta f(r)$
1 C	0.235	0.137	0.103	0.098	0.034	0.066	0.064
2 C	0.037	0.027	-0.049	0.01	0.076	0.043	-0.066
3 C	0.016	0.031	-0.064	-0.015	0.095	0.04	-0.11
4 C	0.203	0.099	0.049	0.104	0.05	0.077	0.054
5 C	0.177	0.078	0.028	0.099	0.05	0.0745	0.049
6 C	0.094	0.157	0.061	-0.063	0.096	0.0165	-0.159
7 O	-0.314	-0.333	-0.372	0.019	0.039	0.029	-0.02
8 N	-0.211	-0.34	-0.243	0.129	-0.097	0.016	0.226
9 C	0.427	0.46	0.342	-0.033	0.118	0.0425	-0.151
10 N	-0.279	-0.321	-0.363	0.042	0.042	0.042	0
11 C	0.117	0.087	0.07	0.03	0.017	0.0235	0.013
12 C	0.032	-0.076	-0.115	0.108	0.039	0.0735	0.069
13 C	0.367	0.48	0.34	-0.113	0.14	0.0135	-0.253
14 C	0.252	0.133	0.07	0.119	0.063	0.091	0.056
15 N	-0.211	-0.204	-0.242	-0.007	0.038	0.0155	-0.045
16 C	0.39	0.241	0.232	0.149	0.009	0.079	0.14
17 N	-0.26	-0.319	-0.348	0.059	0.029	0.044	0.03
18 C	0.086	0.022	0.014	0.064	0.008	0.036	0.056
19 N	-0.121	-0.188	-0.262	0.067	0.074	0.0705	-0.007
20 C	0.086	0.02	0.013	0.066	0.007	0.0365	0.059
21 N	-0.123	-0.192	-0.263	0.069	0.071	0.07	-0.002

The potential energy density (V_{BCP}), electronic energy density (H_{BCP}), kinetic energy density (G_{BCP}), the electron density (ρ_{BCP}), Laplacian of electron density ($\nabla^2 \rho_{BCP}$), and ellipticity (δ) are parameters (Weinhold 2012; Yildiko et al., 2021). Molecular graphs of the MTPPN compound are shown in Figure 3. MTPPN compound was analyzed in the program and reported in Table 3.

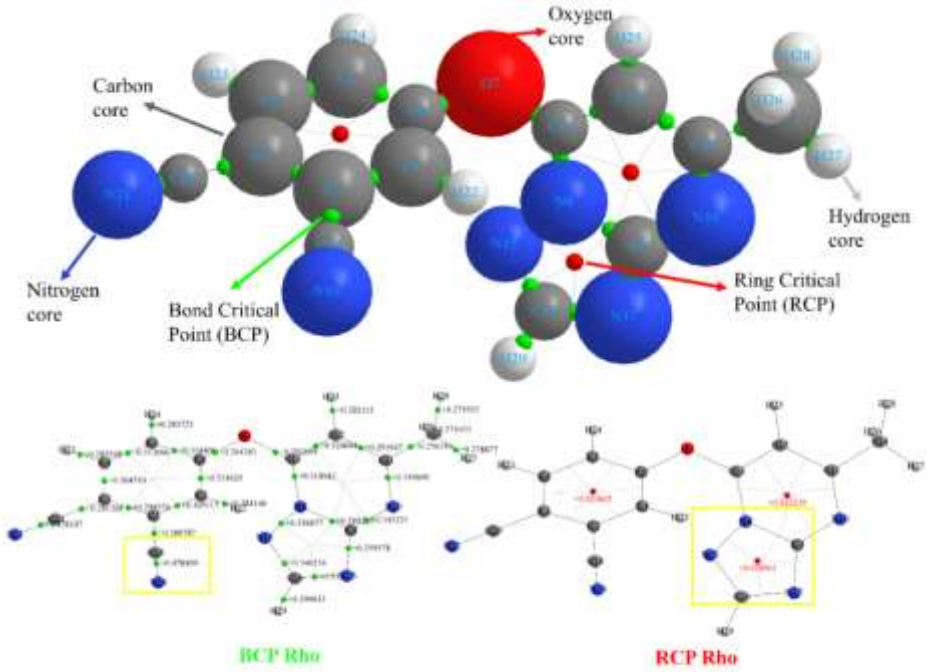

Figure 3. Molecular graphs of MTPPN compound

Table 3. The parameters of the MTPPN compound (all in a.u.)

Contact	ρ_{BCP}	$\nabla^2\rho_{BCP}$	G_{BCP}	V_{BCP}	H_{BCP}	δ
C1 - C2	0.305	-0.837	0.1	-0.409	0.309	0.23
C2 - C3	0.299	-0.804	0.094	-0.388	0.295	0.234
C3 - C4	0.305	-0.841	0.098	-0.405	0.308	0.213
C6 - O7	0.264	-0.282	0.292	-0.655	0.363	0.034
N8 - C13	0.319	-0.870	0.231	-0.68	0.449	0.237
N8 - C9	0.289	-0.722	0.197	-0.575	0.378	0.154
C9 - N10	0.345	-1.086	0.19	-0.652	0.462	0.152
C12 - C13	0.325	-0.94	0.128	-0.491	0.363	0.332
N10 - C11	0.350	-0.961	0.274	-0.789	0.515	0.135
O7 - C13	0.293	-0.428	0.312	-0.732	0.419	0.054
N8 - N15	0.357	-0.627	0.197	-0.551	0.354	0.103
C16 - N17	0.338	-1.016	0.206	-0.665	0.460	0.144
C9 - N17	0.36	-1.125	0.207	-0.696	0.488	0.216
N15 - C16	0.346	-0.94	0.275	-0.785	0.510	0.213
C2 - C18	0.281	-0.769	0.079	-0.351	0.272	0.071
C18 - N19	0.478	-0.25	0.8	-1.664	0.863	0.023
C20 - N21	0.478	-0.26	0.797	-1.659	0.862	0.023
C3 - C20	0.281	-0.769	0.081	-0.354	0.273	0.080
C1 - H22	0.284	-0.987	0.037	-0.320	0.284	0.020
C4 - H23	0.286	-1.00	0.035	-0.321	0.285	0.015

It has been pointed out that the bond critical point property Rho (ρ_{BCP}) and ring critical point property Rho (ρ_{RCP}) values of the MTPPN compound are higher in the regions where the nitrogen core are attached. As a result of the analysis, it was determined that nitrogen atoms have a high electron density. In this case, the bond interactions in these regions of the molecule are expected to be strong.

ADME analysis of MTPPN

The absorption, distribution, metabolism, and excretion of a compound in the human body are related to its ADME properties. ADME, which forms the pharmacological profile of a drug molecule, is very significant in the assessment of its pharmacological activities. Today, many online tools and offline software programs are existing that help us predict this drug candidate behavior (Nisha et al., 2016). ADME studies are used in drug production in order to select the right promising compounds and to minimize the risk of new-term drugs as much as possible. There should be a harmonious balance between pharmacokinetic and pharmacodynamic properties to be predicted in these studies (Abdelhady et al., 2019). Referring to Lipinski's rule of 5, the LogP and molecular weight of an existing orally selected drug should be greater than 5 and 500, respectively. It should be capable of accepting less than 10 hydrogen bonds and donating less than 5 hydrogen bonds (Lin et al., 2003). Online servers such as SwissADME (http://www.swissadme.ch/index.php) were used. Check the chemo-informatics and biological properties of these ligand molecules.

PSA value is 99.89 <140 (Topological), A^2 ABS is between 74.54-82.42% (Figure 4 and Table 4). Among all values, the compound seems to have preferable permeability to the other molecule.

Molecular docking simulations of MTPPN

Molecular docking is useful for studying the ligand-receptor binding mechanism and for understanding the interaction of binding modes (Bernetti et al., 2017).

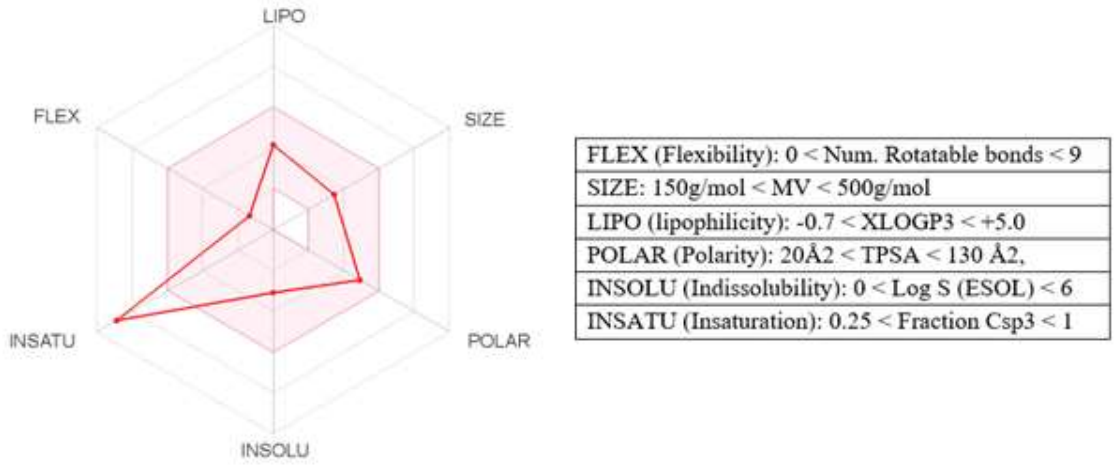

Figure 4. Color regions and pharmacological parameters of MTPPN

Table 4. Potansiyel drug parameters of the title molecules

Molecule	Lipophilicity con. logP	Physicochemical properties								
		MR[a]	% ABS[b]	TPSA[c] (A^2)	H-bond don.	H-bond acc.	Rot. bond	MW[d] g/mol	Aromatic heavy atoms	Heavy atoms
MTPPN	1.54	71.69	74.54	99.89	0	6	2	276.25	15	21

[a]MR, molar refractivity; [b]%ABS: percentage of absorption (%ABS = 109-[0.345 × TPSA]; [c]MW, molecular weight; [d]TPSA, topological polar surface area;

Crystallographic structures of enzymes obtain from the Research Collaboratory for Structural Bioinformatics (RCSB) protein database (PDB) (see http // www.rcsb.org/pdb). Here, molecular docking was performed to acquire preferential binding sites of ligands with the receptor and to largely approve the empirical investigation. As a result of this study, which included a compound and 3 sets of enzymes, 3 good docking results were reached (see Table 5). These ligands placed in the catalytic active area of the enzyme were analyzed based on binding affinity and docking results in interaction mode. However, the best binding affinity score in terms of molecular structure was observed in AChE and BChE enzymes.

Table 5. The best binding affinity scores (kcal/mol) of compounds in the catalytic sites of enzymes

Code	Docking Score		
	AChE (PDB: 4M0E)	BChE (PDB:6SAM)	α-GLY (PDB:3A4A)
MTPPN	-7.864	-6.848	-5.511

The structural similarity of the protein structure to the native ligand increases this value. Protein dynamics play an important role in creating the conditions for how proteins interact with certain derivatives to create complexes that can improve or inhibit their biological functions. Since AChE is in the binding internal area of proteins, sophisticated proximity was obtained compared to other enzymes.

After catching the optimal distance pose in the whole ligand-enzyme insertion study, the binding modes were investigated to figure out the inhibition mechanisms. The proximity number for binding proximity was calculated docking scores.

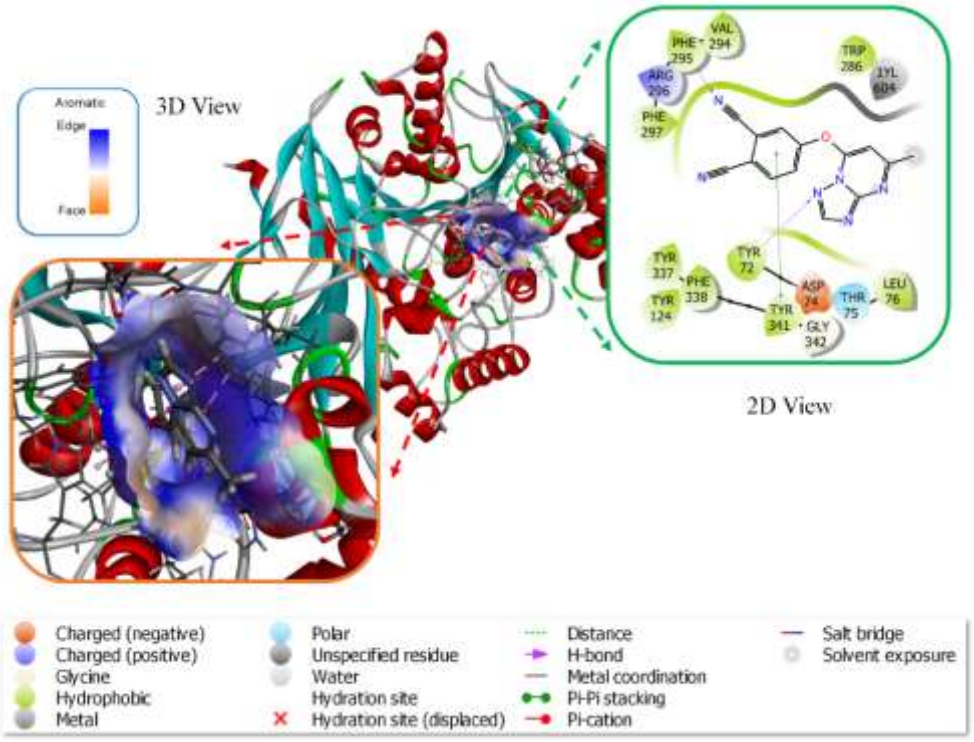

Figure 5. 2D view of MTPPN - AChE enzyme interactions and 3D view of the aromatic surface on the receptor

Figures 5-7 show the 3D and 2D interaction of 4-((5-methyl-[1,2,4]triazolo[1,5-a]pyrimidin-7-yl)oxy)phthalonitrile (MTPPN) – AChE, MTPPN – BchE and MTPPN - α-GLY insertion study (see Table 6).

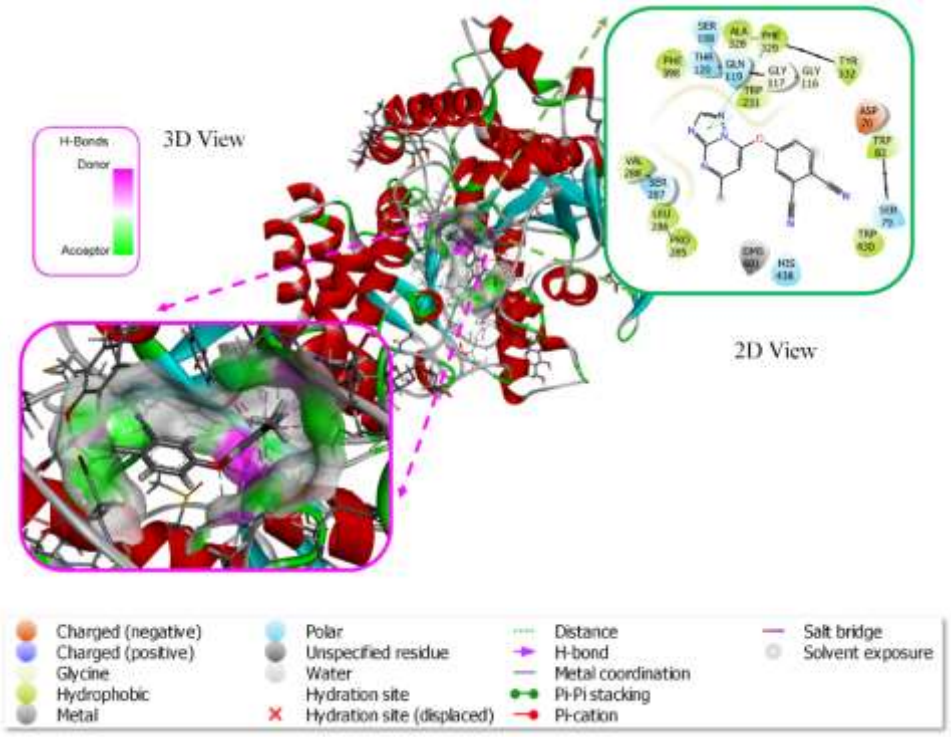

Figure 6. 2D view of MTPPN - BChE enzyme interactions and 3D view of hydrogen bond donor/acceptor surface on the receptor

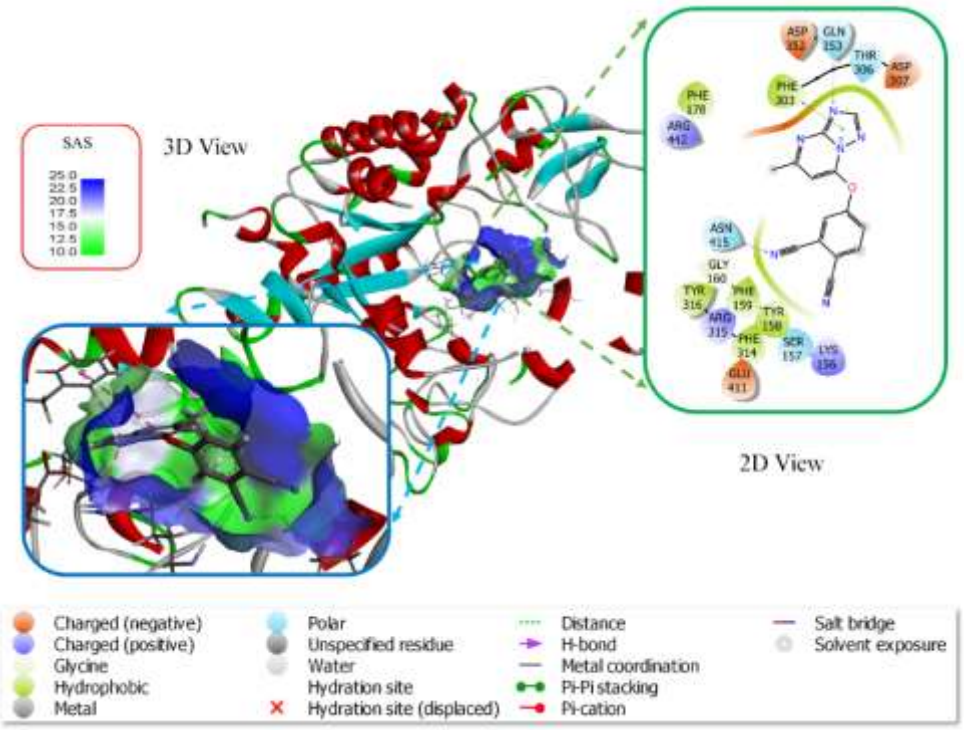

Figure 7. 2D view of MTPPN - α-GLY enzyme interactions and 3D view of the SAS surface on the receptor

Table 6. Bonding mechanisms of MTPPN - AChE, MTPPN - BChE and MTPPN - α-GLY

Enzymes	Codes	Bonds length (Å)	Types of bonding	Bonding points
AChE	PHE-295	1.84	Conventional Hydrogen Bond	Nitrogen
	TYR-72	2.08		Nitrogen of pyrazole
	VAL-294	2.66	Carbon Hydrogen Bond	Nitrogen of phthalonitrile
	LEU-76	4.52	π -alkyl attached	Center of pyrazole ring
	LEU-76	5.40		Center of pyrimidine ring
	TYR-341	3.99	π - π stacking attached	Center of benzene ring
	TRP-286	5.95		Center of benzene ring
	TYR-341	5.56	π - π T-shaped	Center of pyrimidine ring
	TYR-341	5.63		Center of pyrazole ring
	TYR-124	5.67		Center of benzene ring
BChE	SER-198	2.70	Conventional Hydrogen Bond	Nitrogen of pyrazole
	LEU-286	2.59	Carbon Hydrogen Bond	Nitrogen of pyrimidine
	GLY-116	2.71		Bridge oxygen
	GLY-116	4.21	Amid- π stacking attached	Center of pyrimidine ring
	GLY-116	4.59		Center of pyrazole ring
	LEU-286	5.47	π -alkyl attached	Center of pyrazole ring
	TRP-231	5.30	π - π stacking	Center of pyrazole ring
	TYR-341	5.56		Cnter of pyrimidine ring
	PHE-329	5.26		Center of pyrimidine ring
	PHE-329	5.69	π - π T-shaped	Center of pyrimidine ring
α-GLY	GLN-353	2.13	Conventional Hydrogen Bond	Nitrogen of pyrazole
	ASN-415	2.25		Nitrogen of phthalonitrile
	ASP-307	2.46	Carbon Hydrogen Bond	Hydrogen of pyrazole ring
	ARG-315	3.82	π -cation attached	Center of pyrazole ring
	ARG-315	5.04	π -alkyl attached	Center of benzene ring
	PHE-303	4.13	π- π stacking	Center of pyrazole ring
	PHE-303	5.18		Center of pyrimidine ring

CONCLUSION

As molecular modeling techniques have become essential components of chemical, physical and biological study, the aim here is to describe the basic methodology behind three commonly used techniques. Theoretical studies with DFT calculations (HOMO-LUMO, and Fukui function) were made for each structure. It has been pointed out that the bond critical point property Rho (ρ_{BCP}) and ring critical point property Rho (ρ_{RCP}) values of the MTPPN compound are higher in the regions where the nitrogen core is attached as a result of AIM analysis. In addition, ADME analysis was applied to the special compound belonging to the phthalonitrile group, and its color regions and all values were presented. Finally, molecular docking studies were executed on three different enzymes (AChE, BChE, α-GLY) for this particular compound. Docking scores and receptor models are presented one by one.Here, it was seen that BChE and MTPPN had the highest scores with AChE.

Conflict of Interest

The article authors declare that there is no conflict of interest between them.

Author's Contributions

The authors declare that they have contributed equally to the article.

REFERENCES

Abdelhady AM, Yin H, Rodriguez Lorenc K, Ji Y, 2019. Clinical Pharmacokinetics (ADME). Clinical Pharmacology in Drug Development 8 (S1): 1-101.

Agirtas MS, Ondes MY, Ozdemir S and Okumus V, 2017. DNA cleavage properties and synthesis of metallophthalocyanines with 5-methyl-[1, 2, 4] triazolo [1, 5-a] pyrimidin-7-oxy substituents. Inorganic and Nano-Metal Chemistry, 47 (7): 1097-1102.

Altun K, Yildiko U, Tanriverdi AA, Cakmak I, 2021. Structural and spectral properties of 4-(4-(1-(4-Hydroxyphenyl)-1-phenylethyl) phenoxy) phthalonitrile: Analysis by TD-DFT method, ADME analysis and docking studies. International Journal of Chemistry and Technology, 5 (2):147-155.

Bernetti M, Cavalli A and Mollica L, 2017. In Medchemcomm pp. 534-550.

Bulat FA, Chamorro E, Fuentealba P and Toro-Labbé A, 2004. Condensation of Frontier Molecular Orbital Fukui Functions. The Journal of Physical Chemistry A, 108 (2): 342-349.

BIOVIA Discovery Studio D. SYSTÈMES BIOVIA Corporate Europe 2016, BIOVIA 334 Cambridge Science Park Cambridge CB4 0WN, England http://accelrys.com/products/collaborative-science/biovia-discovery-studio/

De Lile JR, Kang SG, Son YA and Lee SG, 2020. Do HOMO–LUMO Energy Levels and Band Gaps Provide Sufficient Understanding of Dye-Sensitizer Activity Trends for Water Purification? ACS Omega, 5 (25): 15052-15062.

Demircioglu Z, Kastas CA and Buyukgungor O, 2015. Theoretical analysis (NBO, NPA, Mulliken Population Method) and molecular orbital studies (hardness, chemical potential, electrophilicity and Fukui function analysis) of (E)-2-((4-hydroxy-2-methylphenylimino)methyl)-3-methoxyphenol. Journal of Molecular Structure, 1091 (5): 183-195.

Daina A, Michielin O, Zoete V, 2017. SwissADME: a free web tool to evaluate pharmacokinetics, drug-likeness and medicinal chemistry friendliness of small molecules. Scientific Reports, 7: 42717.

Dong Q, Hu N, Yue H, Wang H, 2021. Inhibitory Activity and Mechanism Investigation of Hypericin as a Novel α-Glucosidase Inhibitor. Molecules, 26 (15) :4566.

Frisch MJ, Trucks GW, Schlegel HB, Scuseria GE, Robb MA, Cheeseman JR, Scalmani G, Barone V, Petersson GA, Nakatsuji H, Li X, Caricato M, Marenich AV, Bloino J, Janesko BG, Gomperts R, Mennucci B, Hratchian HP, Ortiz JV, Izmaylov AF, Sonnenberg JL, Williams, Ding F, Lipparini F, Egidi F, Goings J, Peng B, Petrone A, Henderson T, Ranasinghe D, Zakrzewski VG, Gao J, Rega N, Zheng G, Liang W, Hada M, Ehara M, Toyota K, Fukuda R, Hasegawa J, Ishida M, Nakajima T, Honda Y, Kitao O, Nakai H, Vreven T, Throssell K, Montgomery Jr. JA, Peralta JE, Ogliaro F, Bearpark MJ, Heyd JJ, Brothers EN, Kudin KN, Staroverov VN, Keith TA, Kobayashi R, Normand J, Raghavachari K, Rendell AP, Burant JC, Iyengar SS, Tomasi J, Cossi M, Millam JM, Klene M, Adamo C, Cammi R, Ochterski JW, Martin RL, Morokuma K, Farkas O, Foresman JB, Fox DJ, 2016. Gaussian 16 Rev. C.01, Wallingford, CT.

Hashimoto H, Hattori K, Yamada T and Kobayashi T, 2001. Electro-Absorption Spectroscopy And Semi-Empirical Molecular Orbital Calculations Of Polar Retinoid Analogues. International Journal of Modern Physics B, 15 (28n30): 3773-3776.

Ilyas RA, Sapuan SM, Asyraf MRM, Dayana DAZN, Amelia JJN, Rani MSA, Norrrahim MN, Nurazzi NM, Aisyah HA, Sharma S, Ishak MR, Rafidah M and Razman MR, 2021. Polymer Composites Filled with Metal Derivatives: A Review of Flame Retardants. Polymers, 13 (11): 1701.

Ledoux I and Zyss J, 1994. Nonlinear Organic Molecules And Materials For Optoelectronic Devices. Journal of Nonlinear Optical Physics & Materials, 03 (03): 287-316.

Lin J, Sahakian DC, de Morais SM, Xu JJ, Polzer RJ and Winter SM, 2003. The role of absorption, distribution, metabolism, excretion and toxicity in drug discovery. Current topics in medicinal chemistry, 3 (10): 1125-1154.

Liu H, Zhang H, Xu X and Zhang L, 2021. The Opto-Electronic Functional Devices Based on Three-Dimensional Lead Halide Perovskites. Applied Sciences, 11 (4) 1453.

Madakbaş S, Çakmakçı E and Kahraman MV, 2013. Preparation and thermal properties of polyacrylonitrile/hexagonal boron nitride composites. Thermochimica Acta, 552: 1-4.

Madhavi Sastry G, Adzhigirey M, Day T, Annabhimoju R, Sherman W, 2013. Protein and ligand preparation: parameters, protocols, and influence on virtual screening enrichments. Journal of Computer-Aided Molecular Design, 27: 221-234.

Mendiratta S, Lee C-H, Usman M and Lu K-L, 2015. Metal-organic frameworks for electronics: emerging second order nonlinear optical and dielectric materials. Science and Technology of Advanced Materials, 16 (5): 054204-054204.

Nemykin VN and Lukyanets EA, 2010. Synthesis of substituted phthalocyanines. ARKIVOC, 2010 (1): 136-208.

Nisha CM, Kumar A, Nair P, Gupta N, Silakari C, Tripathi T and Kumar A, 2016. Molecular Docking and In Silico ADMET Study Reveals Acylguanidine 7a as a Potential Inhibitor of β-Secretase. Advances in Bioinformatics, 2016: 9258578.

Oida, 2006. In Optica Industry Report. Optica, 2006 pp. 3.

Pathak S, Saha GC, Abdul Hadi MB and Jain NK, 2021. Engineered Nanomaterials for Aviation Industry in COVID-19 Context: A Time-Sensitive Review. Coatings, 11 (4): 382.

Pendás ÁM, Gatti C, 2021. 3 Quantum theory of atoms in molecules and the AIMAll software. Complementary Bonding Analysis, 43. https://doi.org/10.1515/9783110660074-003

Priya Madhuri K and John NS, 2022. In Design, Fabrication, and Characterization of Multifunctional Nanomaterials, ed. S. Thomas, N. Kalarikkal and A.R. Abraham. Elsevier, pp. 401-448.

Tan M, Temel S, 2012. Alternative Feed Crops. Ataturk University Agricultural Faculty Course Publications No: 246, pp. 195-207, Erzurum-Turkey.

Tekes AT, Ata AC, Tanriverdi AA, Cakmak I, 2021. Insilico Molecular Docking Studies of THBF Compound: TD-DFT Simulations and Drug Design. Journal of the Institute of Science and Technology, 11 (4): 2955-2966.

Van Mourik T, Buhl M and Gaigeot MP, 2014. Density functional theory across chemistry, physics and biology. Philosophical Transactions of the Royal Society A: Mathematical, Physical and Engineering Sciences, 372 (2011): 20120488-20120488.

Weinhold F, 2012. Natural bond critical point analysis: Quantitative relationships between natural bond orbital-based and QTAIM-based topological descriptors of chemical bonding. Journal of Computational Chemistry, 33 (30): 2440-2449.

Yang Y, Díaz Palencia JL, Wang N, Jiang Y and Wang DY, 2021. Nanocarbon-Based Flame Retardant Polymer Nanocomposites. Molecules (Basel, Switzerland), 26 (15): 4670.

Yankova R, Genieva S, Halachev N and Dimitrova G, 2016. Molecular structure, vibrational spectra, MEP, HOMO-LUMO and NBO analysis of Hf(SeO3)(SeO4)(H2O)4. Journal of Molecular Structure, 1106: 82-88.

Yildiko U and Tanriverdi AA, 2021. Synthesis and characterization of pyromellitic dianhydride based sulfonated polyimide: Survey of structure properties with DFT and QTAIM. Journal of Polymer Research, 29 (1): 19.

Zangwill A, 2014. The education of Walter Kohn and the creation of density functional theory. Archive for History of Exact Sciences, 68 (6): 775-848.